The Risk of Exposure to Diagnostic Ultrasound in Postnatal Subjects

Thermal Effects

William D. O'Brien, Jr, PhD, Cheri X. Deng, PhD, Gerald R. Harris, PhD, Bruce A. Herman, MS, Christopher R. Merritt, MD, Naren Sanghvi, MS, James F. Zachary, DVM, PhD

Abbreviations
AIUM, American Institute of Ultrasound in Medicine; ALARA, as low as reasonably achievable; FDA, Food and Drug Administration; HIFU, high-intensity focused ultrasound; I_{SATA}, spatial-average temporal-average intensity; $I_{SPPA.3}$, derated spatial-peak pulse-average intensity; $I_{SPTA.3}$, derated spatial-peak temporal-average intensity; MI, mechanical index; NCRP, National Council on Radiation Protection and Measurements; NEMA, National Electrical Manufacturers Association; ODS, output display standard; ROC, radius of curvature; TI, thermal index; TIB, thermal index for bone; TIC, thermal index for cranial bone; TIS, thermal index for soft tissue

Received April 12, 2007, from the Bioacoustics Research Laboratory, Department of Electrical and Computer Engineering (W.D.O.), and Department of Pathobiology (J.F.Z.), University of Illinois, Urbana, Illinois USA; Department of Biomedical Engineering, Case Western Reserve University, Cleveland, Ohio USA (C.X.D.); US Food and Drug Administration, Center for Devices and Radiological Health, Rockville, Maryland USA (G.R.H., B.A.H.); Department of Radiology, Thomas Jefferson University Hospital, Philadelphia, Pennsylvania USA (C.R.M.); Focus Surgery Inc, Indianapolis, Indiana USA (N.S.). Revision requested April 18, 2007. Revised manuscript accepted for publication December 4, 2007.

We thank Gail ter Haar, PhD, DSc, for bringing to our attention references 18 and 30, which provided the Table 2 summary, and Kullervo Hynynen, PhD, for assisting with the identification of Table 3 entries. This work was supported in part by National Institutes of Health grant R37EB002641 (Dr O'Brien).

Address correspondence to William D. O'Brien, Jr, PhD, Bioacoustics Research Laboratory, Department of Electrical and Computer Engineering, University of Illinois, 405 N Mathews, Urbana, IL 61801 USA.
E-mail: wdo@uiuc.edu

CME *Article includes CME test*

This review evaluates the thermal mechanism for ultrasound-induced biological effects in postnatal subjects. The focus is the evaluation of damage versus temperature increase. A view of ultrasound-induced temperature increase is presented, based on thermodynamic Arrhenius analyses. The hyperthermia and other literature revealed data that allowed for an estimate of a temperature increase threshold of tissue damage for very short exposure times. This evaluation yielded an exposure time extension of the 1997 American Institute of Ultrasound in Medicine *Conclusions Regarding Heat* statement (American Institute of Ultrasound in Medicine, Laurel, MD) to 0.1 second for nonfetal tissue, where, at this exposure time, the temperature increase threshold of tissue damage was estimated to be about 18°C. The output display standard was also evaluated for soft tissue and bone cases, and it was concluded that the current thermal indices could be improved to reduce the deviations and scatter of computed maximum temperature rises. *Key words*: Arrhenius analysis; nonfetal tissue; output display standard; temperature increase threshold; thermal mechanism.

I. Introduction

Whenever ultrasonic energy is propagated into an attenuating material, such as soft tissues and bone, the amplitude of the wave decreases with distance. This attenuation results in an overall loss in the energy of the wave, which is due to absorption and scattering. Absorption is a mechanism representing that portion of the wave's energy lost by its conversion into heat; scattering can be thought of as that portion that changes direction, some of which is reflected as

echoes producing the images seen on the screen of the scanner. Because the medium interrogated is capable of absorbing energy with the resultant production of heat, a temperature increase may occur as long as the rate at which heat is produced is greater than the rate at which the heat is removed or dissipated.[1,2] The increase in temperature produced by ultrasound can be calculated using mathematical modeling techniques,[3–5] which are detailed later in this section, and has been estimated for a variety of exposure conditions in vivo.[6]

The principal ultrasound-induced thermal effect studies have focused on embryonic/fetal effects for which there is a large body of literature.[7] Hyperthermia is a proven teratogen in experimental animals[8,9] and, although controversial,[10] is considered by some investigators to be a human teratogen under certain circumstances.[11] Because heat generated by ultrasound is a known phenomenon, the question of impact due to a thermal interaction is relevant.

However, the task herein is the assessment of nonfetal thermal effects for which there is little direct literature evaluation relative to diagnostic ultrasound exposure conditions, that is, microsecond pulse durations, a derated spatial-peak temporal average intensity ($I_{SPTA.3}$) less than or equal to 720 mW/cm^2, and either a mechanical index (MI) less than or equal to 1.9 or a derated spatial-peak pulse-average intensity ($I_{SPPA.3}$) less than or equal to 190 W/cm^2. The output display standard (ODS)[12–14] was developed to address two biophysical indices relative to diagnostic ultrasound exposures; therefore, ODS-based temperature increase computations are often used to assess nonfetal thermal conditions.

When ultrasound induces a temperature increase, both its temporal and spatial aspects must be considered. Thus, the following discussion will focus on temporal and spatial issues but mainly under nonfetal thermal conditions.

Temporal Effects

Healthy cellular activity depends on chemical reactions occurring at the proper location at the proper rate. The rates of chemical reactions and thus of enzymatic activity are temperature dependent. The overall effect of temperature on enzymatic activity is described by the relationship known as the 10°C temperature coefficient, or Q_{10} rule.[15] Many enzymatic reactions have a Q_{10} near 3, which means that for each 10°C increase in temperature, enzymatic activity increases by a factor of 3; a more physical description of rate-dependent temperature effects is the Arrhenius activation energy concept.[16–19] A consequence of a temperature increase is an increase in biochemical reaction rates. However, when the temperature becomes sufficiently high (ie, approximately ≥45°C), significant enzyme denaturation occurs.[20] Subsequently, enzymatic activity decreases and ultimately ceases, which has a significant impact on cell structure and function.

If damage occurs during exposure of tissue(s) to elevated temperature, the extent of damage will be dependent on the duration of the exposure as well as on the temperature increase achieved. Detrimental effects in vitro are generally noted at temperatures of 39°C to 43°C, if maintained for a sufficient time period; at higher temperatures (>44°C), denaturation of proteins can occur.[21] These effects have been documented in experimental studies of heat-induced cell death in cultures of normal and cancerous cell lines. The lethal (100% destruction) dose (LD_{100}) for HeLa cells exposed to different temperatures for differing durations ranged from 41°C for a 96-hour duration to 46°C for a 30-minute duration.[22,23] These findings are analogous to the time-temperature relationship (LD_{50}) that describes the destruction of sarcoma 180 tumor cells in mice[23,24] from 42°C for a 2-hour duration to 46°C for a 7.5-minute duration.

These observations suggest a logarithmic relationship between time and temperature for death due to a temperature increase. Dickson and Calderwood[25] have indicated a similar relationship for time versus temperature for thermally induced death of tumors and normal animal and human tissues.

An empirical formula, based on a large number of studies involving the thermotolerance of cells and tumors relates the time, t (in minutes), required to produce an isoeffect (eg, a given amount of cell killing) to the time (t_{43}) that would be required had the exposure occurred at a reference temperature of 43°C, that is,

$$t_{43} = t\,R^{(43-T)}, \quad (1)$$

where T is the temperature in °C; $R = 0.5$ for $T > 43$°C; and $R = 0.25$ for $T \leq 43$°C.[16–19] Theoretical considerations based on reaction kinetics (thermodynamic Arrhenius analyses) lead to the prediction that the temperature dependence of the rate of protein denaturation is determined primarily by the activation energy. The quantity R is an expression of the relative increase in reaction rate for a 1°C increase in temperature. The rationale for there being two "R" values is based on the empirical determinations of R for a number of biological systems and end points.[17–19,26] In these systems, R values ranged from 0.4 to 0.8, with 0.5 being the most common value, for temperatures above 43°C. The few studies performed at temperatures of 43°C or lower indicate that the R value is approximately half the value obtained at the higher temperatures.

Equation 1, the empirical relationship derived by Sapareto and Dewey,[17] can be used to ascribe an equivalent t_{43} value to any combination of temperature and exposure duration. It also follows that any given biological effect due to hyperthermia can be characterized by the t_{43} value of the causative exposure. The lowest t_{43} value giving rise to some effect would be considered the threshold.

Miller and Ziskin[27] estimated that the t_{43} value was greater than 1 minute for each teratologic observation in their study (the lowest t_{43} value for any effect was 1.9 minutes for the production of exencephaly in the mouse[28]). Rearranging Equation 1, and assuming that $R = 0.25$ (for temperatures ≤43°C), yields

$$t = t_{43}\, 4^{(43 - T)}. \quad (2)$$

Miller and Ziskin[27] used $t_{43} = 1$ minute for fetal tissues, that is,

$$t = 4^{(43 - T)}, \quad (3)$$

and the American Institute of Ultrasound in Medicine (AIUM) *Conclusions Regarding Heat*[29] (Table 1) used Equation 3 ($t_{43} = 1$ minute) to indicate that there have been no significant adverse biological effects observed due to temperature increases less than or equal to those represented by the line defined by this equation (Figure 1); the applicable exposure durations ranged between 1 and 250 minutes.

For nonfetal tissues, a range of t_{43} values has been reported. Results for breast[30] and other tissues[18] are summarized for a variety of end points in Table 2. It should be noted that some of the data were garnered using animal models, whose baseline temperatures were higher than 37°C, implying that the temperature increase necessary to achieve a particular thermal dose would have been lower than would be the case with humans.[31,32] Adjustments might have to be made to deduce the t_{43} values applicable to human beings. Also, in using these values in Equations 1 and 3 to establish a time-temperature safety threshold for diagnostic exposures, it should be noted that many were found from in situ studies in which the temperature increase and heated volume were not very well characterized. Also, at the cellular level, there may not be a well-defined threshold for certain thermal effects, as is shown in cell culture studies in which these variables were well controlled.[26,33]

Equations 1–3 define a temperature-time (temperature-exposure duration) boundary line. On the basis of the empirical evidence discussed in this report, it appears that this boundary line could serve as a guide for determining whether an adverse biological effect due to hyperthermia would be likely. Points representing (combinations of) temperature elevations and exposure durations falling below this boundary would be considered unlikely to produce any harm; exposure conditions represented by points falling above this boundary would have a significant possibility of thermal damage.

Figure 1 shows the temperature-time curves for 4 values of t_{43} (Equation 1). The lower curve (t_{43} = 1 minute) represents that estimated for fetal tissues for t longer than 1 minute.[27,29] This curve has a change of slope at 1 minute because of the change in the value of R ($R = 0.5$ for $T > 43$°C, and $R = 0.25$ for $T \leq 43$°C). The other 3 curves, based on t_{43} values (10, 100, and 240 minutes) in Table 2, represent nonfetal tissues that are less sensitive to tissue damage from temperature. Note that the temperature values for an exposure duration of 1 minute are 43.0°C, 46.3°C, 49.6°C, and 50.9°C for t_{43} values of 1, 10, 100, and 240 minutes, respectively. Based on the values in Table 2, the plotted line for t_{43} = 1 minute represents a conservative, tissue-nonspecific boundary for assessing thermal safety for nonfetal exposures.

For shorter exposure times, the hyperthermia literature shows only a limited number of data points representing the t_{43} thermal dose for exposure durations of less than 1 minute. Table 3 contains a compilation of threshold-based data that have been reported for single-burst exposure durations as short as 100 milliseconds. These data are graphically shown in Figure 2. Also germane to the thermal-dose issue for exposures of less than a few seconds are the single-burst in vivo threshold lesion studies that have been conducted in brain[34,45,46] and liver.[47–49] The threshold lesion curve for cat brain can be described approximately by the expression $I^2t = 16 \times 10^4\ W^2s/cm^4$ for exposure durations between 0.3 milliseconds and 100 seconds. The threshold-lesion curve for cat and rabbit liver is described by the expression $I^2t = 21.2 \times 10^4\ W^2s/cm^4$ for exposure durations between 3 milliseconds and 35 seconds. I is the spatial peak intensity (in W/cm^2), and t is the exposure duration (in seconds). One point to be noted here is that liver has a slightly higher threshold than brain, consistent with the t_{43} thermal dose trend for brain and liver in Table 2. A sec-

Table 1. American Institute of Ultrasound in Medicine Conclusions Regarding Heat[29]

Approved March 26, 1997

1. Excessive temperature increase can result in toxic effects in mammalian systems. The biological effects observed depend on many factors, such as the exposure duration, the type of tissue exposed, its cellular proliferation rate, and its potential for regeneration. Age and stage of development are important factors when considering fetal and neonatal safety. Temperature increases of several degrees Celsius above the normal core range can occur naturally; there have been no significant biological effects observed resulting from such temperature increases except when they were sustained for extended time periods.
   a. For exposure durations up to 50 hours, there have been no significant adverse biological effects observed due to temperature increases less than or equal to 2°C above normal.
   b. For temperature increases greater than 2°C above normal, there have been no significant adverse biological effects observed due to temperature increases less than or equal to $6 - (\log_{10} t/0.6)$, where t is the exposure duration ranging from 1 to 250 minutes. For example, for temperature increases of 4°C and 6°C, the corresponding limits for the exposure duration t are 16 and 1 minute, respectively.
   c. In general, adult tissues are more tolerant of temperature increases than fetal and neonatal tissues. Therefore, higher temperatures and/or longer exposure durations would be required for thermal damage.
2. The temperature increase during exposure of tissues to diagnostic ultrasound fields is dependent on (1) output characteristics of the acoustic source such as frequency, source dimensions, scan rate, power, pulse repetition frequency, pulse duration, transducer self-heating, exposure time, and wave shape and (2) tissue properties such as attenuation, absorption, speed of sound, acoustic impedance, perfusion, thermal conductivity, thermal diffusivity, anatomic structure and nonlinearity parameter.
3. For similar exposure conditions, the expected temperature increase in bone is significantly greater than in soft tissues. For this reason, conditions where an acoustic beam impinges on ossifying fetal bone deserve special attention due to its close proximity to other developing tissues.
4. Calculations of the maximum temperature increase resulting from ultrasound exposure in vivo should not be assumed to be exact because of the uncertainties and approximations associated with the thermal, acoustic, and structural characteristics of the tissues involved. However, experimental evidence shows that calculations are capable of predicting measured values within a factor of 2. Thus, it appears reasonable to use calculations to obtain safety guidelines for clinical exposures where temperature measurements are not feasible. To provide a display of real-time estimates of tissue temperature increases as part of a diagnostic system, simplifying approximations are used to yield values called thermal indices.* Under most clinically relevant conditions, the soft tissue thermal index, TIS, and the bone thermal index, TIB, either overestimate or closely approximate the best available estimate of the maximum temperature increase (ΔT_{max}). For example, if TIS = 2, then $\Delta T_{max} \leq 2$°C.
5. The current FDA regulatory limit for $I_{SPTA.3}$ is 720 mW/cm^2. For this, and lesser intensities, the best available estimate of the maximum temperature increase in the conceptus can exceed 2°C.
6. The soft tissue thermal index, TIS, and the bone thermal index, TIB, are useful for estimating the temperature increase in vivo. For this purpose, these thermal indices are superior to any single ultrasonic field quantity such as the derated spatial-peak temporal-average intensity, $I_{SPTA.3}$. That is, TIS and TIB track changes in the maximum temperature increases, ΔT_{max}, thus allowing for implementation of the ALARA principle, whereas $I_{SPTA.3}$ does not. For example,
   a. At a constant value of $I_{SPTA.3}$, TIS increases with increasing frequency and with increasing source diameter.
   b. At a constant value of $I_{SPTA.3}$, TIB increases with increasing focal beam diameter.

*The thermal indices are the nondimensional ratios of the estimated temperature increases to 1°C for specific tissue models (see the *Standard for Real-Time Display of Thermal and Mechanical Acoustic Output Indices on Diagnostic Ultrasound Equipment*[12]).

ond point is that for the brain threshold studies, an estimate was made of lesion temperature increase ΔT, yielding, at 6 MHz, $\Delta T/I$ estimates (interpolated from Figure 4 of Lerner et al[34]) of 0.086°C-, 0.13°C-, and 0.16°C-cm^2/W for pulse durations of 1, 10, and 100 seconds, respectively. Combining these $\Delta T/I$ estimates with $I^2t = 16 \times 10^4$ W^{2}s/cm^4, and assuming that a cat's core temperature is 39°C,[2] yields the 3 temperature-time data points that are listed in Table 3 and plotted as open triangles in Figure 2.

These data (Table 3) suggest that for nonfetal soft tissue and for scanning conditions consistent with conventional B-mode ultrasound examinations for which the exposure durations at the same in situ locations would be less than a few seconds (see section IV), the allowable maximum temperature increase, ΔT, could be relaxed relative to values represented by the conservative boundary line for longer exposures of nonfetal tissue. Specifically, by solving Equation 1 for $\Delta T = T - 37$ and using a value for t_{43} of 8 minutes, a

$$\Delta T = 9 - \frac{\log_{10}(t/60)}{0.3}$$

line (Figure 3, top of the step) can be used as a conservative boundary for nonfetal exposure durations less than 5 seconds, where ΔT is in °C and t is in seconds, and for which there have been no significant adverse biological effects observed due to temperature values smaller than or equal to this line. A continuation of this line (Figure 3, bottom of the step) for exposure durations greater than 5 seconds follows the t_{43} = 1 minute line, which meets the line described in paragraph 1b of the March 26, 1997, AIUM *Conclusions Regarding Heat* statement[29] (Table 1) at 60 seconds. Specifically, the t_{43} = 1 minute line is

$$\Delta T = 6 - \frac{\log_{10}(t/60)}{0.3}$$

between 5 and 60 seconds, and

$$\Delta T = 6 - \frac{\log_{10}(t/60)}{0.6}$$

for times greater than 60 seconds. For example, for temperature increases (Figure 3, bold line) of 18.3°C, 14.9°C, 12.6°C, 9.6°C, and 6.0°C, the corresponding limits for the exposure durations t are 0.1, 1, 5(–), 5(+), and 60 seconds, respectively. In

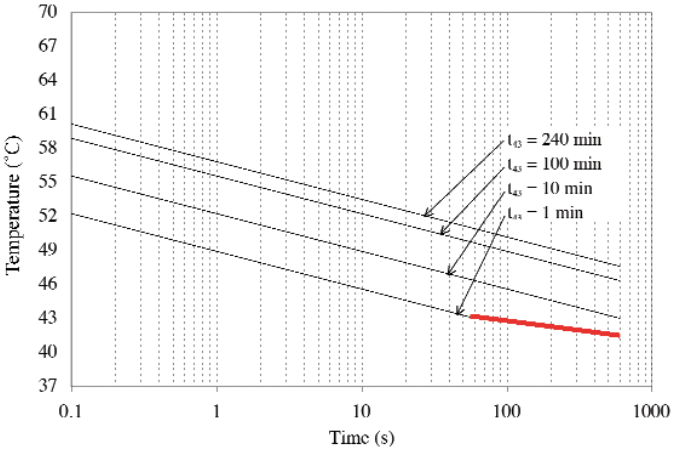

Figure 1. Temperature-time curves for 4 values of t_{43} (see Equation 1, for which $R = 0.5$ for $T > 43$°C and $R = 0.25$ for $T \leq 43$°C). The bold t_{43} = 1 minute red line shows the lower exposure duration range (applicable to 1 minute) of the March 26, 1997, AIUM *Conclusions Regarding Heat* statement.[29]

summary, the temperature increase (bold) line (relative to 37°C) in Figure 3 is mathematically represented as

$$\text{(4a)} \quad \Delta T = 9 - \frac{\log_{10}(t/60)}{0.3} \quad 0.1 < t < 5$$

$$\text{(4b)} \quad \Delta T = 6 - \frac{\log_{10}(t/60)}{0.3} \quad 5 < t < 60$$

$$\text{(4c)} \quad \Delta T = 6 - \frac{\log_{10}(t/60)}{0.6} \quad 60 \leq t,$$

where t is exposure duration in seconds.

Table 2. Thermal Dose t_{43} Values for Various Tissues[18,30]

Tissue	Species	t_{43}, min
Muscle, fat	Pig	240
Skin	Human, rat, mouse	210
Esophagus	Pig	120
Cartilage	Rat, mouse	120
Breast	Human	100
Bladder	Dog, rabbit	80
Small intestine	Rat, mouse	40
Colon	Pig, rabbit	30
Liver	Dog, rabbit	30
Brain	Cat, dog	25
Kidney	Mouse	20

Effect of Treated Volume Size

There appears to be little information about the effect of the heated tissue volume on the threshold of thermal damage to cells. The reason is perhaps that regardless of the tissue volume heated, the threshold for a cell is unlikely to vary as long as the temperature is the same, and the physiologic factors are unchanged. However, the volume of tissue that is damaged and the location of the damage appear to have a critical impact from the point of view of well-being of the patient. During whole-body hyperthermia treatments, where temperatures of cancer patients were elevated to 42°C for 2 hours, severe liver complications resulting in patient death were observed.[50] However, temperatures of 41.8°C appeared to be safe for the whole-body exposure.[51]

Focused ultrasound hyperthermia treatments of tumors have shown that significantly higher temperatures than 41.8°C can be induced locally (volume dimensions were several centimeters) in tumors and their surrounding normal tissues without any significant side effects.[52,53] In these treatments, patients felt intolerable pain before observable damage was done to the normal tissues. Thus, patient pain appears to be a protective mechanism for significant tissue damage. However, this is not the case in organs that lack pain sensors, for example, the brain.

It is important to note that organs such as the kidney, liver, and lung are built structurally for redundancy; you can lose a large proportion of the tissue volume in these organs without appreciable changes in normal organ function as monitored by serum biochemical analyses. Also, the regenerative ability of a tissue listed in Table 2 varies; as an example, loss of cells in the intestinal mucosa is much less significant than loss of cells in the brain.

Furthermore, it has also been noted that even if small tissue volumes are destroyed, it may not have an impact on the well-being of the patient. Linke et al[54] showed that rabbits could tolerate small regions of tissue necrosis in the liver and kidney, induced by high-power focused ultrasound bursts that were unlikely to cause an overall impact for the kidney or liver as noted above. There are clinical data available on thermal tissue ablation by high-intensity focused ultrasound (HIFU) of the entire or partial prostate gland,[55–58] kidney,[59] liver,[60] breast,[60] and uterus.[61] These data show no significant side effects on the well-being of patients and illustrate that if critical organs or critical structures within organs are spared, limited damage occurs. Thermal ablation by focused ultrasound in these

Table 3. Temperature-Time Threshold–Based Data for Various Biological Materials

Figure 2 Symbol	Time, s	Temp, °C	Material	Reference
Open triangle*	1	73.4	Cat brain in vivo	Lerner et al[34]
Open triangle*	10	55.4	Cat brain in vivo	Lerner et al[34]
Open triangle*	100	45.4	Cat brain in vivo	Lerner et al[34]
Filled circle	1.4	65	Cat brain in vivo	Lele[35]
Filled circle	1.8	64	Cat brain in vivo	Lele[35]
Filled circle	2.5	63	Cat brain in vivo	Lele[35]
Filled circle	3	65	Cat brain in vivo	Lele[35]
Filled triangle	10	53	Rabbit brain in vivo	Vykhodtseva et al[36]
Filled triangle	30	48	Rabbit brain in vivo	McDannold et al[37]
Filled triangle	30	47.8	Rabbit brain in vivo	Chen et al[38]
Filled square	9	60.2	Rat brain in vivo	Pond[39]
Filled square	3	63.7	Rat brain in vivo	Pond[40]
Open diamond	30	47.2	Rabbit muscle in vivo	McDannold et al[41]
Open diamond	30	47.5	Rabbit muscle in vivo	Cheng et al[42]
Open circle	180	51	Dog prostate in vivo	Peters et al[43]
Open square	1	57	Baby hamster kidney cells in vitro	Borrelli et al[33]
Dashed line†	0.1	64.5	Multiple tissue thresholds	Lele[44]
Dashed line‡	770	41.5	Multiple tissue thresholds	Lele[44]
Shaded line†	60	46.2	Multiple in vitro thresholds	Henle[16]
Shaded line‡	840	42.9	Multiple in vitro thresholds	Henle[16]

*Interpolated.
†Minimum time value is that reported in the article.
‡Maximum time value was truncated to fit the curve.

organs is produced using extracorporeal and intracavitary transducers. The HIFU waves propagate through several intervening tissue layers and blood vessels during each ultrasound exposure burst. The HIFU exposure burst can be 1 to 20 seconds long followed by an on-off period of 1 to 90 seconds. The process of HIFU exposure continues for a long period (70–140 minutes) to treat 30 to 40 cm^3 of tissue of a selected organ. These results indicate no significant effects immediately in the biochemical blood analysis or over a long period of regular posttreatment follow-up over 5 years. The documented major biological effects appear to be local and not systemic. On the other hand, even a small volume of damage to critical brain tissue may have serious consequences,[62] whereas a person can tolerate a larger volume of tissue damage in another, less critical part of the brain.[63,64] The eye is another organ where even a small amount of tissue damage may be unacceptable.

II. Output Display Standard

In the mid-1980s, the US Food and Drug Administration (FDA) initiated the regulatory process for diagnostic ultrasound equipment and set application-specific intensity limits that could not be exceeded.[65,66] Unfortunately, these limits were not based on safety considerations. Rather, they were based on relative risk for regulatory decision-making purposes and were obtained from measurements of the acoustic output of diagnostic ultrasound systems that had been entered into interstate commerce before May 28, 1976, the date when the Medical Devices Amendments were enacted.[67] In the early 1990s, the FDA implemented the *Standard for Real-Time Display of Thermal and Mechanical Indices on Diagnostic Ultrasound Equipment* (commonly called the ODS).[12,65,68,69] While the ODS[12] did not specify upper limits, the FDA's implementation[65] of the ODS stipulated regulatory upper limits of 720 mW/cm^2 for the derated (0.3 dB/cm-MHz) $I_{SPTA.3}$ and either 1.9 for the MI or 190 W/cm^2 for the derated (0.3 dB/cm-MHz) $I_{SPPA.3}$. There is, however, an exception for ophthalmic applications, for which $I_{SPTA.3}$ less than or equal to 50 mW/cm^2 and MI less than or equal to 0.23 are specified.[65] In addition, the FDA[65] requires the manufacturer to justify

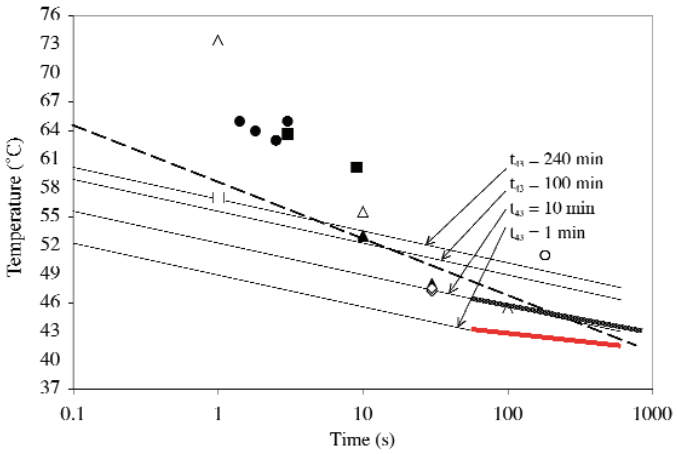

Figure 2. Temperature-time curves (Figure 1) plus the following threshold data: filled circle, cat brain; open triangle, cat brain (estimated; see section I); filled triangle, rabbit brain; filled square, rat brain; open diamond, rabbit muscle; open circle, dog prostate; open square, baby hamster kidney cells; dashed line, multiple tissue thresholds; and shaded line (just above the bold t_{43} = 1 minute red line), multiple in vitro thresholds. Details are listed in Table 3.

thermal indices (TIs) greater than 6. The ODS has been revised,[13,14] but the FDA's regulatory upper limits have not changed.

The purpose of the ODS[12–14] is to provide the capability for users of diagnostic ultrasound equipment to operate their systems at levels much higher than previously had been possible to have greater diagnostic capabilities. In doing so, the possibility for harm to the patient was hypothesized because of the potential for higher output levels. Therefore, the ODS requires that two biophysical indices be provided so that the

Figure 3. Temperature-time curves (see Figure 2) plus a bold red line that represents a conservative boundary for nonfetal exposure durations, particularly for exposure durations less than 5 seconds.

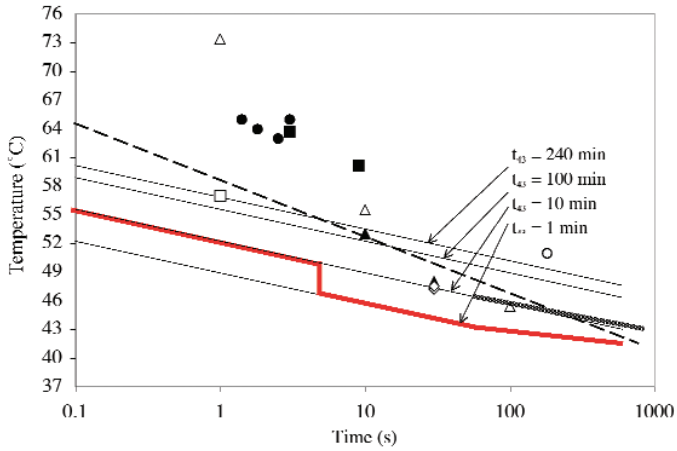

equipment operator has displayed information available to make appropriate clinical decisions, namely, benefit versus risk, and to implement the ALARA (as low as reasonably achievable) principle.[70] The two biophysical indices are the TI and the MI. The TI provides information about tissue-temperature increase and the MI provides information about the potential for cavitation. This chapter addresses the thermal mechanism and the closely related TI.

The basic TI definition is[14]

$$TI = \frac{W_O}{W_{DEG}} \quad (5)$$

where W_0 is the source power of the diagnostic ultrasound system, and W_{DEG} is the source power required to increase the tissue temperature by 1°C under very specific and conservative conditions. Three different TIs were developed to address 3 different tissue models and 2 different scan modes, that is, the thermal index for soft tissue (TIS), the thermal index for bone (TIB), and the thermal index for cranial bone (TIC). The unscanned mode is typically used clinically for spectral Doppler and M-mode, in which the ultrasound beam remains stationary for a period of time. Also, the unscanned-mode TIS and TIB are the only TI quantities that attempt to estimate temperature increases at locations other than at or near the source surface.

The following computational evaluation addresses the accuracy of the unscanned-mode TIS for circular[4] and rectangular[5] sources.

Figure 4. Dimensions of the 33 rectangular aperture cases investigated.

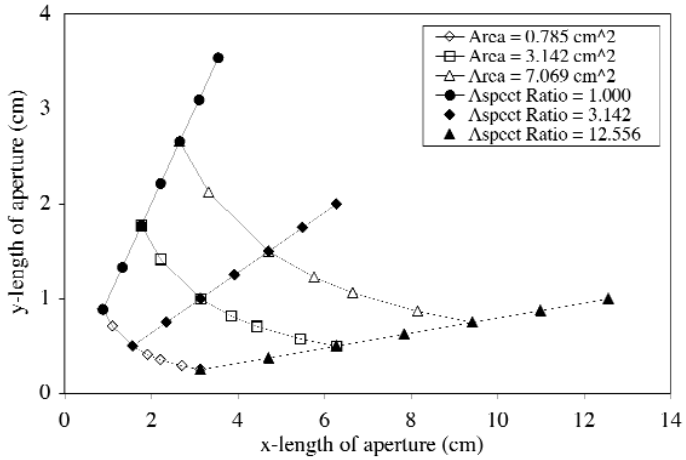

For the circular sources,[4] 3 source diameters (1, 2, and 4 cm) and 8 transmit *f*-numbers (radius of curvature [ROC]/source diameter = 0.7, 1.0, 1.3, 1.6, 2.0, 3.0, 4.0, and 5.0) were evaluated at 8 frequencies (1, 2, 3, 4, 5, 7, 9, and 12 MHz), yielding 192 cases. For the rectangular sources,[5] 33 1-dimensional focused rectangular-aperture cases were investigated (Figure 4) for which the aperture's *x* length direction is the axis that is focused (*y* length direction not focused) by an appropriate ROC to yield 3 *f*-numbers (ROC/*x* length = 1, 2, and 4). Six frequencies (1, 3, 5, 7, 9, and 12 MHz) were evaluated (99 combinations/frequency), yielding 594 cases.

For all 786 cases, the medium was assumed to be homogeneous in terms of both acoustic and thermal properties. The attenuation coefficient (also referred to as a derating factor) and absorption coefficient were both 0.3 dB/cm-MHz; density was 1000 kg/m^3; propagation speed was 1540 m/s; tissue perfusion length was 1 cm; and tissue thermal conductivity was 6 mW/cm-°C. These were the values used in the ODS[12–14] and the values used herein for the evaluation of the unscanned-mode TIS. They were also the values used to compute the maximum steady-state temperature increase (ΔT_{max}) and its axial location. Also, all results reported herein are based on the derated $I_{SPTA.3}$ of 720 mW/cm^2, the FDA's regulatory limit.[65]

Figures 5 and 6 directly compare the 192 circular-source ΔT_{max}-TIS computed results as a function of frequency and *f*-number, respectively. The TIS generally underestimates (is less than) ΔT_{max} for *f*-numbers less than or equal to 2, conditions for which ΔT_{max} is less than or equal to 0.3°C and TIS is less than or equal to 0.4. This suggests that for transmit *f*-numbers less than or equal to 2, the TIS would not need to be displayed according to the ODS display requirements. With the exception of the longer-focus, larger-diameter, higher-frequency sources, the TIS generally tracks ΔT_{max} for *f*-numbers greater than or equal to 3. These exceptions suggest a breakdown of the ODS procedures for calculating the TIS under the mentioned conditions.

Figures 7 and 8 directly compare the 594 rectangular-source ΔT_{max}-TIS computed results as a function of frequency and *f*-number, respectively. The TIS overestimates (is greater than) ΔT_{max} for all but

1 of the cases, namely, 1 MHz, *f*/1, area = 0.785 cm^2; aspect ratio = 1.57; ΔT_{max} = 0.153°C; and TIS = 0.148.

Location of the Maximum Steady-State Temperature Increase

The ODS process does not specify the location of ΔT_{max}. Figures 9 and 10 show the relationship between ΔT_{max} and its location (axial distance) for the circular and rectangular sources, respectively, as a function of *f*-number (the same 3 *f*-numbers are shown for direct comparison). Figures 11 and 12 show the relationship between ROC and the axial distances to the locations of ΔT_{max} for the circular and rectangular sources, respectively, as a function of *f*-number. For all 786 cases, the axial distances to the locations of ΔT_{max} are less than the ROC that locates the geometric focus location. For the lower *f*-number cases, the axial distance locations of ΔT_{max} move closer to the geometric focus as frequency increases. However, for the higher *f*-number cases in each frequency set, the axial distance locations of ΔT_{max} jump to near the transducer surface when *f* is greater than or equal to 3 MHz. This behavior, also reported by Thomenius,[71] becomes more prevalent at higher frequencies and larger source diameters. Thus, the ΔT_{max} location is not necessarily near the skin surface; in many cases, the ΔT_{max} location is near the skin surface, but it is always between the geometric focus and the skin surface.

Temporal-Spatial Dependency of the Temperature Increase

In scanned modes, the focal energy is distributed over a large area and hence will usually have lower temporal-average intensities than unscanned modes. With the recent introduction of real-time 3-dimensional scanners, the focal energy will be distributed (scanned) over 2 dimensions; that should result in further reduction in spatially distributed focal intensities. However, there will be an added concern of near-field heating. Near-field heating could be exacerbated by transducer self-heating.[72] At this time, we believe that the development of a new index to cover these cases is not indicated in view of the regulatory mechanisms that are already in place for limiting transducer surface temperatures.

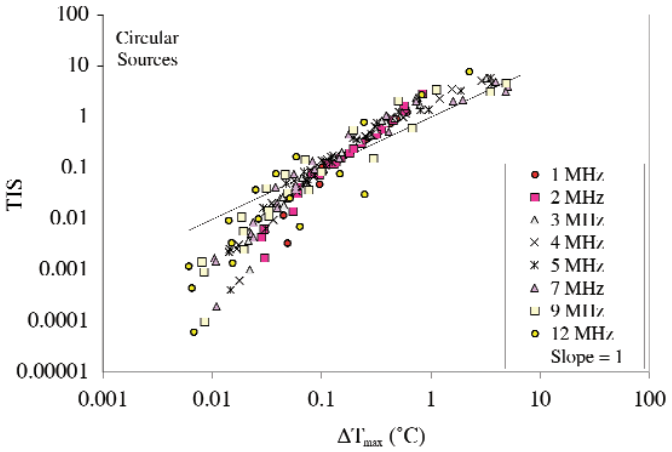

Figure 5. Paired maximum steady-state temperature increase ΔT_{max} versus unscanned-mode TIS for 192 circular sources grouped by frequency under the condition that the derated $I_{SPTA.3}$ is 720 mW/cm^2.

The ODS process does not take into account the temporal-spatial dependency of the temperature increase. An evaluation of the temporal-spatial dependency of the temperature increase was conducted for the circular sources of 3 source diameters (1, 2, and 4 cm) at 2 frequencies (2 and 7 MHz) for 5 *f*-numbers (*f*/1, *f*/2, *f*/3, *f*/4, and *f*/5); Figure 13 shows $t_{80\%}$, the time when the temperature increase reaches 80% of its steady-state value at that axial distance, for 2 source diameters (1 and 4 cm). Each $t_{80\%}$ profile follows the same general pattern as a function of axial distance. For each of the 7-MHz cases, the axial distances of the minimum $t_{80\%}$ values are, in general, near the

Figure 6. Paired maximum steady-state temperature increase ΔT_{max} versus unscanned-mode TIS for 192 circular sources grouped by *f*-number under the condition that the derated $I_{SPTA.3}$ is 720 mW/cm^2.

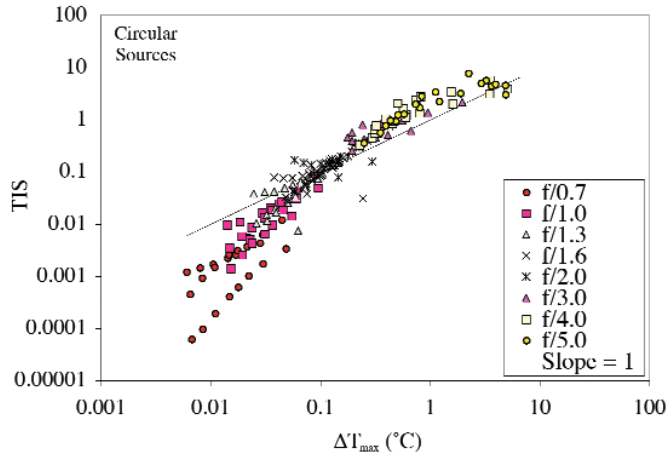

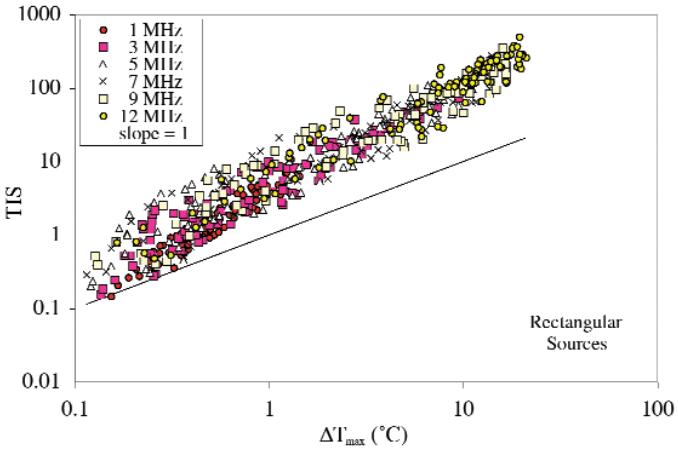

Figure 7. Paired maximum steady-state temperature increase ΔT_{max} versus unscanned-mode TIS for 594 rectangular sources grouped by frequency under the condition that the derated $I_{SPTA.3}$ is 720 mW/cm^2.

respective focal regions. However, for the 2-MHz cases, the axial distances of the minimum $t_{80\%}$ values tend not to be near the respective focal regions but rather closer to the transducer. Also, the minimum $t_{80\%}$ values increase as a function of increasing *f*-number and decrease as a function of increasing frequency. The global minimum $t_{80\%}$ values are 97.2 and 59.7 seconds for the 15 2-MHz and 15 7-MHz cases, respectively, both of which are for the 1-cm-diameter, *f*/1 cases.

Better Indices Possible

The TIs in use today were developed more than 15 years ago.[12] While the ODS has been revised twice,[13,14] the TI expressions have not changed. Figures 5–8 indicate that there could be improvements to reduce the scatter of computed results and change the mean slopes. There has been one effort to improve the unscanned-mode TIS. The set of results that was computed for the 594 rectangular-source cases was evaluated to see whether an improved TI expression could be developed.[5] This evaluation yielded two new TIS expressions:

$$\text{TIS}_{\text{new(1)}} = \frac{W_o^{0.85} f_c^{0.58}}{169 \cdot A_{\text{aprt}}^{0.33}} \quad (6)$$

$$\text{TIS}_{\text{new(2)}} = \frac{W_o^{0.73} f_c^{0.62}}{130}, \quad (7)$$

where W_0 is the source power (in mW); f_c is the center frequency (in MHz); and A_{aprt} is the active aperture area (in cm^2) (Figure 14). In both models, only the source power and frequency need to be measured; they can be measured adequately.[73] The only difference between $\text{TIS}_{\text{new(1)}}$ and $\text{TIS}_{\text{new(2)}}$ is the degree of agreement with ΔT_{max} that might be desired. The spread (variance) about the TIS = ΔT_{max} line is greater for $\text{TIS}_{\text{new(2)}}$ than for $\text{TIS}_{\text{new(1)}}$. It should be noted that these two new TIS expressions were developed under the condition for which $I_{SPTA.3}$ = 720 mW/cm^2; the purpose of this evaluation was to show the potential for improvement, not necessarily to suggest that these two new TIS expressions would satisfy all conditions for rectangular sources. There has been no known suggested improvement for circular sources.

Figure 8. Paired maximum steady-state temperature increase ΔT_{max} versus unscanned-mode TIS for 594 rectangular sources grouped by *f*-number under the condition that the derated $I_{SPTA.3}$ is 720 mW/cm^2.

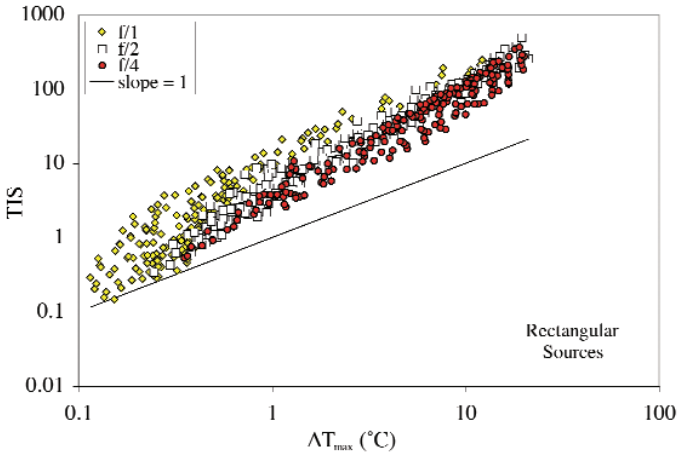

III. Thermal Bioeffects Due to New Technologies

Low-Output Commercial Fracture-Healing System

In 2000, the FDA approved an ultrasound fracture-healing system for healing of nonunions and accelerated healing of fresh fractures. Clinical studies showed the treatment to be effective, although the mechanism of action is still unclear. While not a diagnostic application, it warrants consideration of possible heating from this device. The system uses an unfocused ultrasound transducer with an effective radiating

diameter, *d*, of 2.2 cm and an operating frequency of 1.5 MHz (Table 4). The ultrasound is pulsed with a duration of 200 microseconds and a repetition frequency of 1 kHz, for a duty factor of 20%. The spatial-average temporal-average intensity at the transducer face ($I_{SATA@face}$) is 30 mW/cm^2, and the temporal-average ultrasonic power, *W*, is 117 mW. Using these values, the TIS at the transducer face ($I_{SATA@face}f/210$) is 0.2; also, the TIC [$W/(40d)$] is 1.3. A crude estimate of the TIB,

$$\left(\mathrm{TIB} = \sqrt{4\,W\,I_{SATA\,@\,face}\,10^{-0.06 f z_{B.3}}} \,/\, 50 \right),$$

in which $z_{B.3}$ is taken to be one fifth the distance to the theoretical last axial intensity maximum, yields a value of less than 1.5. These indices were computed using formulas in Table 2-2 of the *Standard for Real-Time Display of Thermal and Mechanical Acoustic Output Indices on Diagnostic Ultrasound Equipment*.[14] From these results, tissue heating does not seem to be a concern for this application.

Transient Temperature Increase During High-Intensity Pulses or Pulse Bursts

In calculating the TIs in the ODS, temporal-average quantities (intensity and power) are used as independent variables in the relevant formulas (Table 2-2 of the *Standard for Real-Time Display of Thermal and Mechanical Acoustic Output Indices on Diagnostic Ultrasound Equipment*[14]), resulting in worst-case indices related to steady-state temperatures. Temporal-average quantities were used under the assumption that the time scale of the acoustic regimen is fast compared to thermal processes. This assumption is reasonable for diagnostic pulses[74] but may not be so for newer techniques using ultrasound radiation force to induce tissue displacement for remote palpation or acoustic streaming.[75–82] These methods can use high-intensity pulses, or bursts of pulses, up to tens[78] or hundreds[77] of milliseconds, in addition to the conventional Doppler pulses.

The question arises as to whether temperatures could increase to possibly hazardous levels during the acoustic pulse or pulse burst.[83] If so, consideration must be given to models that might be used for calculation of the temperature increase. It is also important to understand whether, given current knowledge concerning bioeffects of temperature increases in tissue, a limiting intensity or power can be specified below which the temperature rise is such that there is negligible concern for safety.

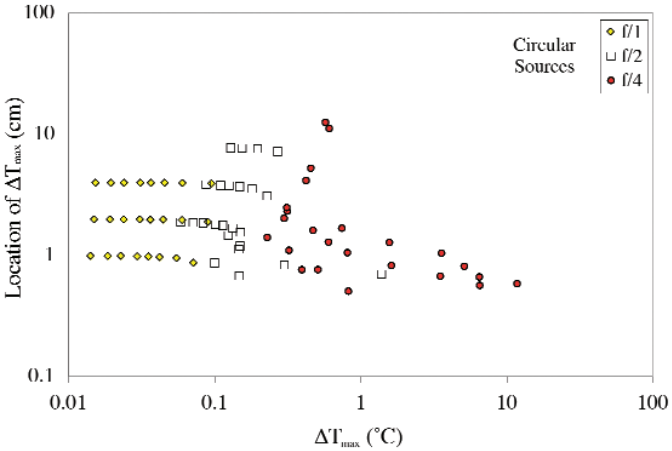

Figure 9. Paired maximum steady-state temperature increase ΔT_{max} versus location (axial distance) of ΔT_{max} for circular sources grouped by *f*-number under the condition that the derated $I_{SPTA.3}$ is 720 mW/cm^2.

Using simple models under conservative assumptions, Herman and Harris[84] concluded that transient temperatures could rise to possibly dangerous levels under certain conditions and pulse regimens that might be encountered during these newer diagnostic ultrasound procedures and with acoustic output held within current FDA limits. The following analysis is taken from Herman and Harris.[84] In their calculations, values of tissue thermal and absorption quantities for tis-

Figure 10. Paired maximum steady-state temperature increase ΔT_{max} versus location (axial distance) of ΔT_{max} for rectangular sources grouped by *f*-number under the condition that the derated $I_{SPTA.3}$ is 720 mW/cm^2.

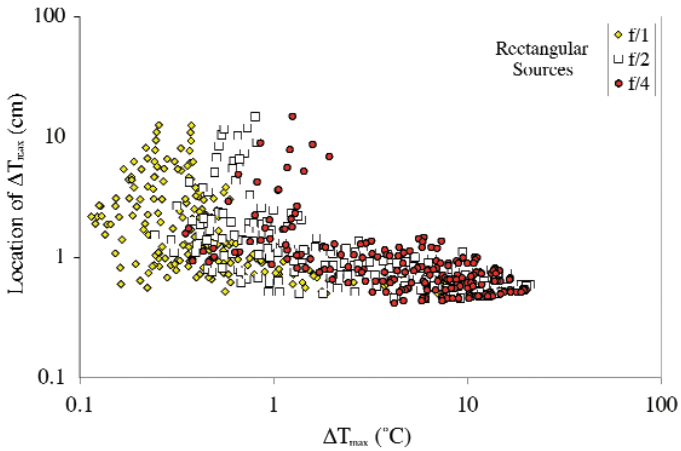

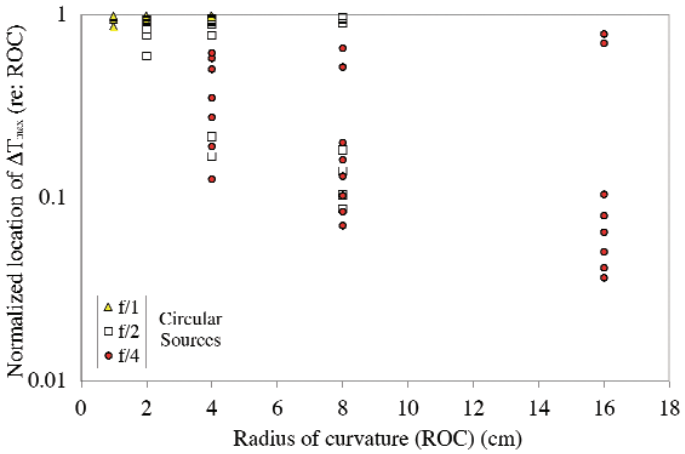

Figure 11. Paired location of the geometric focus (ROC) versus normalized location (axial distance) of ΔT_{max} [(location of ΔT_{max})/ROC] for circular sources grouped by *f*-number.

sue were those assumed in deriving the ODS TIs. Other values used were based on tables from the National Council on Radiation Protection and Measurements (NCRP) criteria.[2] Furthermore, all analyses assumed that the focal diameter was smaller than the perfusion length of soft tissue and that the pulse duration was smaller than the perfusion time constant. Thus, the effects of perfusion were considered negligible.

Figure 12. Paired location of the geometric focus (ROC) versus normalized location (axial distance) of ΔT_{max} [(location of ΔT_{max})/ROC] for rectangular sources grouped by *f*-number.

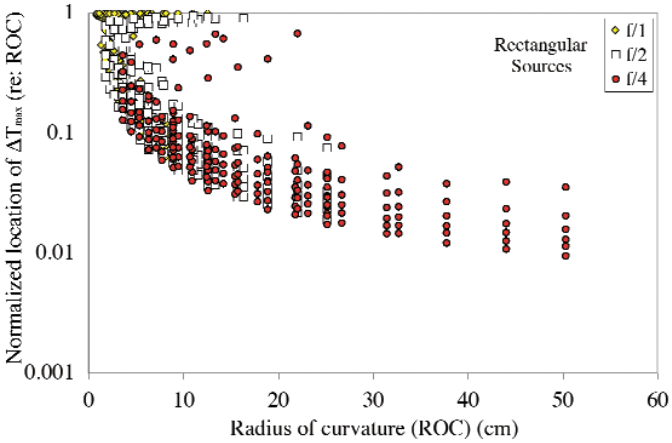

Focus on Bone

Under these assumptions and using the totally absorbing, very thin disk model of the ODS's TIB,[66] the temperature increase ΔT (in degrees Celsius) in bone at the focus for focal diameters from 0.1 to 1 cm and for times less than 250 milliseconds can be expressed as[84]

$$(8) \quad \Delta T = (0.012 + 0.060\, t^{0.487})I,$$

where I (in W/cm^2) is the spatial-peak intensity, temporally averaged over the duration t (in milliseconds), of the high-intensity pulse or pulse burst. This result was derived by using numerical integration of point sources and regression curve fitting.

For example, for t = 200 milliseconds and I = 10 W/cm^2, which are values suggested by Nightingale et al,[77] Equation 8 yields ΔT = 8.0°C. This spatial-peak temporal-average-over-pulse intensity value is possible while maintaining the FDA $I_{SPTA.3}$ limit of 720 mW/cm^2, indicating that such short, high-intensity pulses could result in large temperature increases while also having an MI less than the regulatory limit of 1.9.

Focus on Soft Tissue

To make a conservative calculation of the soft tissue time dependence of temperature at the location of maximum ultrasound intensity, this intensity may be considered characteristic of a broad beam of uniform intensity, *I*. For this case, conductive losses are negligible, and, if the plane wave assumption (Appendix D of the NCRP criteria[2]) for the heat source term is used, the temperature increase (independent of focal diameter by this assumption) is given in chapter 6 of the NCRP criteria[2]:

$$(9) \quad \Delta T = \frac{2\alpha f I t}{c_v},$$

where α is the pressure absorption coefficient in soft tissue (in cm^{-1}MHz^{-1}); f is the frequency (in MHz); c_v is the heat capacity per unit volume of soft tissue (in mW-s/cm^3-°C); and I and t are in W/cm^2 and milliseconds, respectively. This simple result is adequate for soft tissue exposure times less than 250 milliseconds. With α = 0.05 cm^{-1}MHz^{-1} and c_v = 4000 mW-s/cm^3-°C,

(10) $$\Delta T = 2.5 \times 10^{-5} f I t,$$

so only high-intensity levels, high frequencies, and long pulses can produce large temperature increases. For example, for $t = 200$ milliseconds, $I = 10\ \mathrm{W/cm^2}$, $f = 7$ MHz,[77] and $\Delta T = 0.35$°C (4.4% of the temperature increase as calculated when bone is involved).

Temperature and Intensity Limits

Solving the isoeffect relationship in Equation 1 with $R = 0.5$ yields $T = 43 - 1.44 \ln(t/t_{43})$. Then, solving for a temperature increase relative to 37°C, ΔT_{37}, yields

(11) $$\Delta T_{37} = 6 - 1.44 \ln(t/t_{43}).$$

Also, rewriting the formula for the temperature increase in bone in Equation 8 by neglecting the additive constant and approximating the exponent by 0.5 gives

(12) $$\Delta T = 0.06\ t_B^{0.5}\ I,$$

where t_B (in milliseconds) is the duration of the high-intensity pulse or pulse burst, I. (Note: An analytic derivation by Herman and Myers[85] shows that the exponent is very close to 0.5 for t < 250 milliseconds.) By combining Equations 11 and 12, an upper bound on I based on thermal considerations can be calculated:

(13) $$I \le \frac{100 - 24 \ln\left(t/t_{43}\right)}{t_B^{0.5}},$$

where $t_B < 250$ milliseconds.

A question that arises in the application of these results for setting a "safe" thermal dose is what is the lower bound on the exposure time for which they are valid. The data used to derive Equation 1 do not include exposure times below 1 minute,[17] so it is unclear whether they are relevant down to second or millisecond periods. However, in Figure 2 and the accompanying discussion, evidence was presented that exposure times down to approximately 100 milliseconds may be used. In the absence of additional data, a conservative safety analysis would seem to require that limits be imposed that are based on the lowest time t for which Equation 11 is valid, even for shorter times. Therefore, if $t_B < 100$ milliseconds, then t should be 100 milliseconds in Equation 13. If $t_B \ge 100$ milliseconds (but < 250 milliseconds), then $t = t_B$, and Equation 13 becomes

(14) $$I \le \frac{100 - 24 \ln\left(t_B / t_{43}\right)}{t_B^{0.5}}.$$

For example, if $t_{43} = 1$ minute and $t_B = 200$ milliseconds, then $I \le 10\ \mathrm{W/cm^2}$.

Figure 13. Profiles of $t_{80\%}$ as a function of axial distance for the 2-MHz (red) and 7-MHz (blue) cases for 1-cm-diameter (top) and 4-cm-diameter (bottom) circular sources under the condition that the derated $I_{SPTA.3}$ is 720 mW/cm^2.

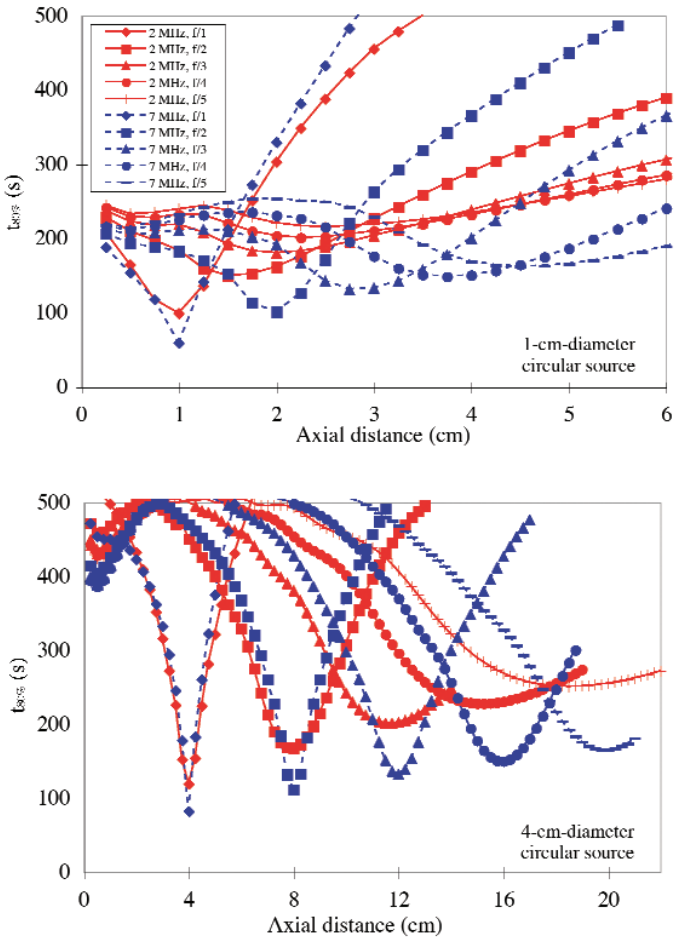

In a similar manner for soft tissue, Equations 10 and 11 can be combined to give

$$(15)\quad I \le \frac{\left[24 - 5.76 \ln\left(t / t_{43}\right)\right] \times 10^4}{f t_B}.$$

Again, if t_B < 100 milliseconds, then t should be 100 milliseconds in Equation 15. For $t_B \ge 100$ and < 250 milliseconds, $t = t_B$, and Equation 15 becomes

$$(16)\quad I \le \frac{\left[24 - 5.76 \ln\left(t_B / t_{43}\right)\right] \times 10^4}{f t_B}.$$

For example, if t_{43} = 1 minute, t_B = 200 milliseconds, and f = 7 MHz, then $I \le 240$ W/cm^2.

Figure 14. Paired maximum steady-state temperature increase ΔT_{max} versus the proposed unscanned-mode $TIS_{new(1)}$ (top) and $TIS_{new(2)}$ (bottom) for rectangular sources grouped by *f*-number under the condition that the derated $I_{SPTA.3}$ is 720 mW/cm^2.

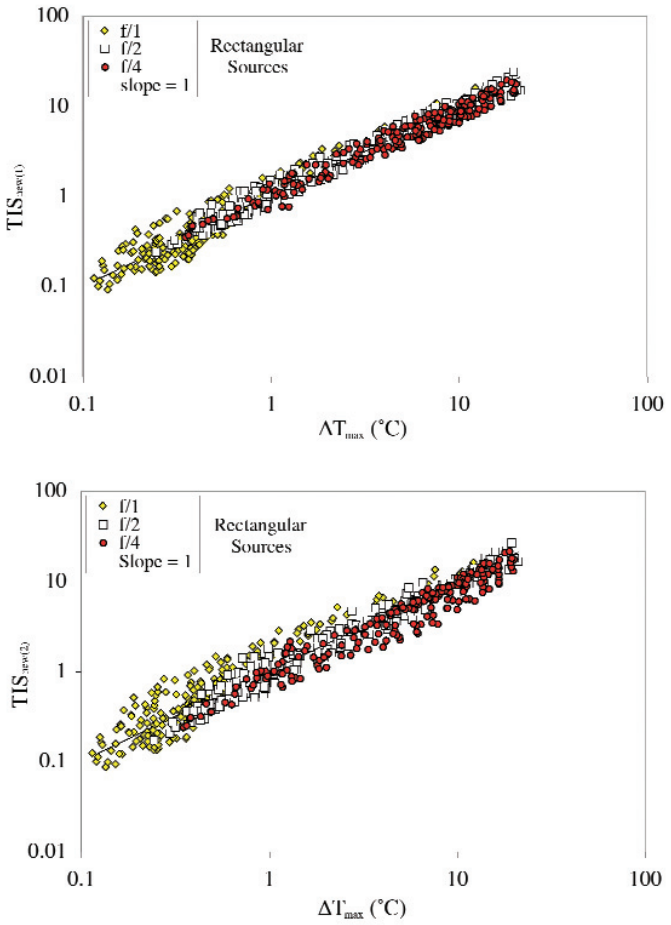

As was discussed in Section I in connection with Equations 1–3, the t_{43} values in Table 2 could be used in Equations 14 and 16 as a basis for establishing intensity-time safety guidelines.

IV. Relationship to Clinical Exposure Conditions

Exposure conditions related to the production of thermal bioeffects in experimental settings are likely to differ from those that exist in the setting of a typical clinical diagnostic examination. These differences will, in general, result in a lower risk of biological effects in clinical practice than those predicted from experimental data.

Real-time B-Mode Imaging

Due to the movement of the transducer and of the structures being imaged during clinical examination, the acoustic field remains fixed over a given structure or volume of tissue for brief periods of time, typically measured in seconds or fractions of a second. Under these conditions, the probability of local tissue or organ heating is small and unlikely to be of clinical significance.

Color or Power Doppler Imaging

As in imaging modes, color Doppler examinations typically involve continuous movement of the transducer (acoustic field) with respect to the tissue or organ being insonated. Due to the movement of the transducer and movement of the structures being imaged during clinical examination, the acoustic field remains fixed over a given structure or volume of tissue for brief periods of time, typically measured in seconds or fractions of a second. Under these conditions, the probability of local tissue or organ heating is small and unlikely to be of clinical significance.

Pulsed Doppler Imaging

Measurements of Doppler spectra typically involve the positioning of a small (2-to 6-mm) Doppler sample volume within the lumen of a vascular structure of interest. To obtain accurate Doppler measurements, the sample volume is directed constantly to a region of interest for several cardiac cycles resulting in dwell times typically in the range of 5 to 10 seconds. Even under these conditions, the probability of local tissue or

organ heating is still small and unlikely to be of clinical significance.

V. Implementing ALARA

A diagnostic ultrasound educational activity was initiated with a workshop in June 1988. This workshop set out certain principles, which resulted in the initiation of a 3-year process involving numerous clinicians, scientists, engineers, and government regulators from many organizations; this group finalized and approved, in 1992, the *Standard for Real-Time Display of Thermal and Mechanical Indices on Diagnostic Ultrasound Equipment*, commonly referred to as the ODS.[12] The purpose of this voluntary standard was to provide the capability for users of diagnostic ultrasound equipment to operate their systems at levels much higher than had been permitted previously to provide the potential for greater diagnostic capabilities; the standard did not specify any upper limits. Thus, potentially, it was possible to do harm to the patient. Therefore, two biophysical indices were provided so that the equipment operator would have real-time information available to make appropriate clinical decisions, namely, benefit versus risk, and to implement the ALARA principle. Thus, the ODS provides for a real-time output display that gives the user information about the potentials for temperature increase (the TI) and mechanical damage (the MI).

Table 4. Acoustic Output Characteristics for a Commercial Fracture-Healing System

Acoustic Quantity	Value
Frequency, MHz	1.5
Transducer area, cm^2	3.88
Effective transducer diameter, cm	2.22
Pulse duration, μs	200
Pulse repetition frequency, kHz	1
Duty factor	0.2
Ultrasonic power, mW	117
I_{SATA} at transducer face, mW/cm^2	30
I_{SAPA} at transducer face, mW/cm^2	150.8
p_r at transducer face, kPa*	67.0
TIS at transducer face	0.2
TIC	1.3

I_{SAPA} indicates spatial-average pulse-average intensity; and p_r, peak rarefactional pressure. Reference: http://www.exogen.com/

*Assuming pressure amplitude is constant over the face.

Following the adoption of the voluntary ODS, the FDA revised its diagnostic ultrasound regulatory guidelines by essentially adopting the ODS. The ODS did not include upper limits, as mutually agreed by all parties (AIUM, National Electrical Manufacturers Association [NEMA], and FDA) at the beginning of the ODS development process. However, as explained by O'Brien et al,[67] the FDA added application-nonspecific guidelines[68,69] as regulatory upper limits that were based on a derated $I_{SPTA.3}$ value of 720 mW/cm^2 and an MI value of 1.9.

To complement the ODS, some professional societies (AIUM/NEMA) developed a brochure[86] to satisfy, in part, the FDA's user-educational requirement.[68,69] The brochure is divided into 3 parts. Part One describes ultrasound-induced bioeffects and why we should be concerned about them. Part Two describes the risks and benefits of conducting diagnostic examinations and introduces the concept of ALARA, that is, ultrasound exposure as low as reasonably achievable. Using the ALARA principle, the intent is to obtain needed diagnostic information with minimum risk to the patient. Part Three describes how to implement the ALARA principle on equipment with and without an output display. This brochure provides only the general principles about ALARA and diagnostic ultrasound equipment because each manufacturer's equipment has somewhat different control features.

The implementation of ALARA throughout the diagnostic ultrasound community has been a failure. It is suggested that one reason for this failure is because of the FDA's upper-limit regulatory controls that have been viewed by the clinical community as safety limits. However, these limits are not based on safety considerations. Therefore, it is recommended that an appropriately representative and knowledgeable group evaluate the current TIs and, if needed, develop improved indices.

VI. Conclusions Regarding Nonfetal Heating

Excessive temperature increases can result in adverse effects in mammalian systems. The biological effects observed depend on many factors, such as the exposure duration, the type of tissue

exposed, its cellular proliferation rate, and its potential for regeneration. Temperature increases of several degrees Celsius above the normal core range can occur naturally; there have been no significant biological effects observed resulting from such temperature increases except when they were sustained for extended time periods.

1. For temperature increases less than or equal to 2°C above normal (ie, 37°C), there have been no significant adverse biological effects observed for durations of temperature elevation up to 50 hours.
2. For temperature increases between 2°C and 6°C above normal, there have been no significant, adverse biological effects observed due to temperature increases less than or equal to

$$6 - \frac{\log_{10}(t/60)}{0.6},$$

where t is the exposure duration in seconds.
3. For temperature increases greater than 6°C above normal, there have been no significant adverse biological effects observed due to temperature increases less than or equal to

$$6 - \frac{\log_{10}(t/60)}{0.3},$$

where t is the exposure duration in seconds. For example, for temperature increases of 9.6°C and 6.0°C, the corresponding limits for the exposure durations t are 5 and 60 seconds, respectively (Figure 15).

Figure 15. Temperature-time line that represents a conservative boundary for nonfetal exposure durations. This line appears as the red line in Figure 3.

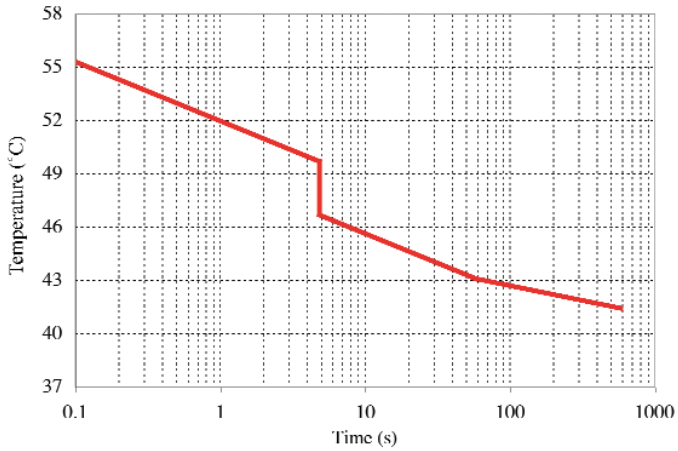

4. For exposure durations less than 5 seconds, there have been no significant adverse biological effects observed due to temperature increases less than or equal to

$$9 - \frac{\log_{10}(t/60)}{0.3},$$

where t is the exposure duration in seconds. For example, for temperature increases of 18.3°C, 14.9°C, and 12.6°C, the corresponding limits for the exposure durations t are 0.1, 1, and 5 seconds, respectively (Figure 15).

Recommendation: Improving Indices

It is recommended that the AIUM, via the Output Standards Subcommittee, take the lead to form an appropriately representative and knowledgeable group to evaluate the current TIs and, if needed, develop improved indices.

Recommendation: Implementing ALARA (Global Recommendation)

It is recommended that the AIUM take the lead to encourage the FDA to develop an open scientifically valid process for assessing the benefits and the risks of removing or modifying the current regulatory limits.

References

1. O'Brien WD Jr. Ultrasonic dosimetry. In: Fry FJ (ed). Ultrasound: Its Applications in Medicine and Biology. New York, NY: Elsevier; 1978:343–391.
2. National Council on Radiation Protection and Measurements. Exposure Criteria for Diagnostic Medical Ultrasound, Part 1: Criteria Based on Thermal Mechanisms. Bethesda, MD: National Council on Radiation Protection and Measurements; 1992. Report 113.
3. Ellis DS, O'Brien WD Jr. The monopole-source solution for estimating tissue temperature increases for focused diagnostic ultrasound. IEEE Trans Ultrason Ferroelectr Freq Control 1996; 43:88–97.
4. O'Brien WD Jr, Ellis DS. Evaluation of the soft-tissue thermal index. IEEE Trans Ultrason Ferroelectr Freq Control 1999; 46:1459–1476.
5. O'Brien WD Jr, Yang Y, Simpson DG. Evaluation of unscanned-mode soft-tissue thermal index for rectangular sources and proposed new indices. Ultrasound Med Biol 2004; 30:965–972.
6. Tarantal AF, O'Brien WD Jr. Discussion of ultrasonic safety related to obstetrics. In: Sabbagha RE (ed). Ultrasound Applied to Obstetrics and Gynecology. 3rd ed. Philadelphia, PA: JB Lippincott Co; 1994:45–56.

7. Abramowicz JS, Barnett S, Duck F, Edmonds P, Hynynen K, Ziskin M. Fetal thermal effects of diagnostic ultrasound. J Ultrasound Med 2008; 27:541–559.

8. Edwards MJ, Wanner RA. Extremes of temperature. In: Wilson JG, Fraser FC (eds). Handbook of Teratology. Vol 1. General Principles and Etiology. New York, NY: Plenum Press; 1977:421–444.

9. Edwards MJ. Hyperthermia as a teratogen: a review of experimental studies and their clinical significance. Teratog Carcinog Mutagen 1986; 6:563–582.

10. Warkany J. Teratology update: hyperthermia. Teratology 1986; 33:365–371.

11. Shepard TH. Human teratogenicity. Adv Pediatr 1986; 33: 225–268.

12. American Institute of Ultrasound in Medicine, National Electrical Manufacturers Association. Standard for Real-Time Display of Thermal and Mechanical Indices on Diagnostic Ultrasound Equipment. Laurel, MD: American Institute of Ultrasound in Medicine; Rosslyn, VA: National Electrical Manufacturers Association; 1992.

13. American Institute of Ultrasound in Medicine, National Electrical Manufacturers Association. Standard for Real-Time Display of Thermal and Mechanical Acoustic Output Indices on Diagnostic Ultrasound Equipment. Rev 1. Laurel, MD: American Institute of Ultrasound in Medicine; Rosslyn, VA: National Electrical Manufacturers Association; 1998.

14. American Institute of Ultrasound in Medicine, National Electrical Manufacturers Association. Standard for Real-Time Display of Thermal and Mechanical Acoustic Output Indices on Diagnostic Ultrasound Equipment. Rev 2. Laurel, MD: American Institute of Ultrasound in Medicine; Rosslyn, VA: National Electrical Manufacturers Association; 2004.

15. Hille B. Ion Channels of Excitable Membranes. Sunderland, MA: Sinauer Associates Inc; 2001.

16. Henle KJ. Arrhenius analysis of thermal responses. In: Strom FK (ed). Hyperthermia in Cancer Therapy. Boston, MA: GK Hall Medical Publishers; 1983:47–53.

17. Sapareto SA, Dewey WC. Thermal dose determination in cancer therapy. Int J Radiat Oncol Biol Phys 1984; 10:787–800.

18. Dewey WC. Arrhenius relationships from the molecule and cell to the clinic. Int J Hyperthermia 1994; 10:457–483.

19. Dewhirst MW, Viglianti BL, Lora-Michiels M, Hanson M, Hoppes PF. Basic principles of thermal dosimetry and thermal thresholds for tissue damage from hyperthermia. Int J Hyperthermia 2003; 19:267–294.

20. Lepock JR. Measurement of protein stability and protein denaturation in cells using differential scanning calorimetry. Methods 2005; 35:117–125.

21. Rosenberg B, Kemeny G, Switzer RC, Hamilton TC. Quantitative evidence for protein denaturation as the cause of thermal death. Nature 1971; 232:471–473.

22. Selawry OX, Goldstein MW, McCormick T. Hyperthermia in tissue-cultured cells of malignant origin. Cancer Res 1957; 17:785–791.

23. Hornback NB. Hyperthermia and Cancer: Human Clinical Trial Experience. Vols I, II. Boca Raton, FL: CRC Press; 1984.

24. Crile G Jr. Heat as an adjunct to the treatment of cancer, experimental studies. Cleve Clin Q 1961; 28:75–89.

25. Dickson JA, Calderwood SK. Temperature range and selective sensitivity of tumors to hyperthermia: a critical review. In: Jain RK, Gullino PM (eds). Thermal Characteristics of Tumors: Applications in Detection Treatment. New York, NY: Annals of the New York Academy of Sciences; 1980: 180–205.

26. Dewey WC, Hopwood LE, Sapareto SA, Gerweck LE. Cellular responses to combinations of hyperthermia and radiation. Radiology 1977; 123:463–474.

27. Miller MW, Ziskin MC Biological consequences of hyperthermia. Ultrasound Med Biol 1989; 15:707–722.

28. Webster WS, Edwards MJ. Hyperthermia and the induction of neural tube defects in mice. Teratology 1984; 29:417–425.

29. American Institute of Ultrasound in Medicine. Conclusions Regarding Heat. Laurel, MD: American Institute of Ultrasound in Medicine; 1997.

30. Lyng H, Monge OR, Bohler PJ, Rofstad EK. Relationships between thermal dose and heat-induced tissue and vascular damage after thermoradiotherapy of locally advanced breast carcinoma. Int J Hyperthermia 1991; 7:403–415.

31. Miller MW, Dewey WC. An extended commentary on "Models and regulatory considerations for transient temperature rise during diagnostic ultrasound pulses" by Herman and Harris (2002). Ultrasound Med Biol 2003; 29:1653–1659.

32. Herman BA, Harris GR. Response to "An extended commentary on 'Models and regulatory considerations for transient temperature rise during diagnostic ultrasound pulses' by Herman and Harris (2002)" by Miller and Dewey (2003). Ultrasound Med Biol 2003; 29:1661–1662.

33. Borrelli MJ, Thompson LL, Cain CA, Dewey WC. Time-temperature analysis of cell killing of BHK cells heated at temperatures in the range of 43.5 degrees C to 57.0 degrees C. Int J Radiat Oncol Biol Phys 1990; 19:389–399.

34. Lerner RM, Carstensen EL, Dunn F. Frequency dependence of thresholds for ultrasonic production of thermal lesions in tissue. J Acoust Soc Am 1973; 54:504–506.

35. Lele PP. Thresholds and mechanisms of ultrasonic damage to "organized" animal tissues. In: Hazzard DG, Litz ML (eds). Symposium on Biological Effects and Characterizations of Ultrasound Sources. Vol 78-8048. Washington, DC: US Department of Health, Education, and Welfare, Food and Drug Administration; 1977:224–239.

36. Vykhodtseva N, Sorrentino V, Jolesz FA, Bronson RT, Hynynes K. MRI detection of the thermal effects of focused ultrasound on the brain. Ultrasound Med Biol 2000; 26:871–880.

37. McDannold N, Vykhodtseva N, Jolesz FA, Hynynen K. MRI investigation of the threshold for thermally induced blood-brain barrier disruption and brain tissue damage in the rabbit brain. Magn Reson Med 2004; 51:913–923.

38. Chen L, Wansapura JP, Heit G, Butts K. Study of laser ablation in the in vivo rabbit brain with MR thermometry. J Magn Reson Imaging 2002; 16:147–152.

39. Pond JB. A Study of the Biological Action of Focused Mechanical Waves (Focused Ultrasound) [thesis]. London, England: London University; 1968.

40. Pond JB. The role of heat in the production of ultrasonic focal lesions. J Acoust Soc Am 1970; 47:1607–1611.

41. McDannold NJ, King RL, Jolesz FA, Hynynen KH. Usefulness of MR imaging–derived thermometry and dosimetry in determining the threshold for tissue damage induced by thermal surgery in rabbits. Radiology 2000; 216:517–523.

42. Cheng HLM, Purcell VT, Bilbao JM, Plewes DB. Prediction of subtle thermal histopathological change using a novel analysis of Gd-DTPA kinetics. J Magn Reson Imaging 2003; 18:585–598.

43. Peters RD, Chan E, Trachtenberg J, et al. Magnetic resonance thermometry for predicting thermal damage: an application of interstitial laser coagulation in an in vivo canine prostate model. Magn Reson Med 2000; 44:873–883.

44. Lele PP. Physical aspects and clinical studies with ultrasonic hyperthermia. In: Strom FK (ed). Hyperthermia in Cancer Therapy. Boston, MA: GK Hall Medical Publishers; 1983: 333–367.

45. Fry FJ, Kossoff G, Eggleton RC, Dunn F. Threshold ultrasonic dosages for structural changes in mammalian brain. J Acoust Soc Am 1970; 48:1413–1417.

46. Dunn F, Fry FJ. Ultrasonic threshold dosages for the mammalian central nervous system. IEEE Trans Biomed Eng 1971; 18:253–256.

47. Chan SK, Frizzell LA. Ultrasonic thresholds for structural changes in the mammalian liver. In: Proceedings of the 1977 Ultrasonics Symposium. Piscataway, NJ: Institute of Electrical and Electronics Engineers; 1977:153–156.

48. Frizzell LA, Linke CA, Carstensen EL, Fridd CW, Thresholds for focal ultrasonic lesions in rabbit kidney, liver, and testicle. IEEE Trans Biomed Eng 1977; 24:393–396.

49. Frizzell LA. Threshold dosages for damage to mammalian liver by high-intensity focused ultrasound. IEEE Trans Ultrason Ferroelectr Freq Control 1988; 35:578–581.

50. Van Der Zee J, Van Rhoon GC, Wike-Hooley JL, Faithfull NS, Reinhold HS. Whole-body hyperthermia in cancer therapy: a report of a phase I–II study. Eur J Cancer Clin Oncol 1983; 19:1189–1200.

51. Robins HI, Dennis WH, Neville AJ, et al. A nontoxic system for 41.8 degrees C whole-body hyperthermia: results of a Phase I study using a radiant heat device. Cancer Res 1985; 45:3937–3944.

52. Lele PP, Goddard J, Blanter M, Thermometric and clinical results of MIT SIMFU (scanned, focussed intensity–modulated ultrasound). In: Sugahara T, Saito M (eds). Hyperthermic Oncology. Vol 1. London, England: Taylor & Francis; 1989:614–716.

53. Harari PM, Hynynen K, Roemer RB, et al. Development of scanned focussed ultrasound hyperthermia: clinical response evaluation. Int J Radiat Oncol Biol Phys 1991; 21: 831–840.

54. Linke CA, Carstensen EL, Frizzell LA, Elbadawi A, Fridd CW. Localized tissue destruction by high-intensity focused ultrasound. Arch Surg 1973; 107:887–891.

55. Sanghvi NT, Foster RS, Bihrle R, et al. Noninvasive surgery of prostate tissue by high-intensity focused ultrasound: an updated report. Eur J Ultrasound 1999; 9:19–29.

56. Uchida T, Ohkusa H, Yamashita H, Nagata Y. High-intensity focused ultrasound (HIFU) for the treatment of localized prostate cancer using the Sonablate 500. In: ter Haar GR, Rivens I (eds). Proceedings of the Fourth International Symposium on Therapeutic Ultrasound. College Park, MD: American Institute of Physics; 2005:3–6.

57. Blana A, Walter B, Rogenhofer S, Wieland W. High-intensity focused ultrasound for the treatment of localized prostate cancer: 5-year experience. Urology 2004; 63:297–300.

58. Gelet A, Chapelon JY, Bouvier R, et al. Transrectal high-intensity focused ultrasound: minimally invasive therapy of localized prostate cancer. J Endourol 2000; 14:519–528.

59. Illing RO, Kennedy JE, Wu F, et al. Preliminary experience using extracorporeal high-intensity focused ultrasound for the treatment of kidney and liver tumours. In: ter Haar GR, Rivens I (eds). Proceedings of the Fourth International Symposium on Therapeutic Ultrasound. College Park, MD: American Institute of Physics; 2005:13–16.

60. Wu F, Wang ZB, Chen WZ, et al. Extracorporeal focused ultrasound surgery for treatment of human solid carcinomas: early Chinese clinical experience. Ultrasound Med Biol 2004; 30:245–260.

61. Stewart EA, Gedroyc WM, Tempany CM, et al. Focused ultrasound treatment of uterine fibroid tumors: safety and feasibility of a noninvasive thermoablative technique. Am J Obstet Gynecol 2003; 189:48–54.

62. Lynn JG, Zwemer RL, Chick AJ, Miller AE. A new method for the generation and use of focused ultrasound in experimental biology. J Gen Physiol 1942; 26:179–193.

63. Heimburger RF. Ultrasound augmentation of central nervous system tumor therapy. Indiana Med 1985; 78:469–476.

64. Guthkelch AN, Carter LP, Cassady JR, et al. Treatment of malignant brain tumors with focused ultrasound hyperthermia and radiation: results of a phase I trial. J Neurooncol 1991; 10:271–284.

65. US Food and Drug Administration. Information for Manufacturers Seeking Marketing Clearance of Diagnostic Ultrasound Systems and Transducers. Rockville, MD: US Food and Drug Administration; 1997.

66. Abbott JG. Rationale and derivation of the MI and TI: a review. Ultrasound Med Biol 1999; 25:431–441.

67. O'Brien WD Jr, Abbott JA, Stratmeyer ME, et al. Acoustic output upper limit proposition: should upper limits be retained? J Ultrasound Med 2002; 21:1335–1341.

68. Center for Devices and Radiological Health, US Food and Drug Administration. Revised 510(k) Diagnostic Ultrasound Guidance for 1993. Rockville, MD: Center for Devices and Radiological Health, US Food and Drug Administration; 1993.

69. Center for Devices and Radiological Health, US Food and Drug Administration. Use of Mechanical Index in Place of Spatial Peak, Pulse Average Intensity in Determining Substantial Equivalence. Rockville, MD: Center for Devices and Radiological Health, US Food and Drug Administration; 1994.

70. National Council on Radiation Protection and Measurements. Implementation of the Principle of as Low as Reasonably Achievable (ALARA) for Medical and Dental Personnel. Bethesda, MD: National Council on Radiation Protection and Measurements; 1990. Report 107.

71. Thomenius KE. Thermal dosimetry models for diagnostic ultrasound. In: Proceedings of the 1990 Ultrasonics Symposium. Piscataway, NJ: Institute of Electrical and Electronics Engineers; 1990:1399–1408.

72. Duck FA, Starritt HC, ter Haar GR, Lunt MJ. Surface heating of diagnostic ultrasound transducers. Br J Radiol 1989; 67:1005–1013.

73. American Institute of Ultrasound in Medicine, National Electrical Manufacturers Association. Acoustic Output Measurement Standard for Diagnostic Ultrasound Equipment. Laurel, MD: American Institute of Ultrasound in Medicine; Rosslyn, VA: National Electrical Manufacturers Association; 2004.

74. Barnett SB, ter Haar GR, Ziskin MC, Rott HD, Duck FA, Maeda K. International recommendations and guidelines for the safe use of diagnostic ultrasound in medicine. Ultrasound Med Biol 2000; 26:355–366.

75. Fatemi M, Greenleaf JF. Ultrasound stimulated vibro-acoustic spectrography. Science 1998; 280:82–85.

76. Fatemi M, Greenleaf JF. Vibro-acoustography: an imaging modality based on ultrasound-stimulated acoustic emission. Proc Natl Acad Sci USA 1999; 96:6603–6608.

77. Nightingale KR, Kornguth PJ, Trahey GE. The use of acoustic streaming in breast lesion diagnosis: a clinical study. Ultrasound Med Biol 1999; 25:75–87.

78. Nightingale KR, Palmeri ML, Nightingale RW, Trahey GE. On the feasibility of remote palpation using acoustic radiation force. J Acoust Soc Am 2001; 110:625–634.

79. Walker WF. Internal deformation of a uniform elastic solid by acoustic radiation force. J Acoust Soc Am 1999; 105: 2508–2518.

80. Shi X, Martin RW, Vaezy S, Kaczkowski P, Crum LA. Color Doppler detection of acoustic streaming in a hematoma model. Ultrasound Med Biol 2001; 27:1255–1264.

81. Von Behren PL, Ramachandran AR, Banjanin ZB, Gueck WJ. High transmit power diagnostic ultrasound imaging. Malvern, PA: Siemens Medical Solutions USA Inc. US patent 6 824 518 B2. November 30, 2004.

82. Clarke L, Edwards A, Pollard K. Acoustic streaming in ovarian cysts. J Ultrasound Med 2005; 24:617–621.

83. Palmeri ML, Nightingale KR. On the thermal effects associated with radiation force imaging of soft tissue. IEEE Trans Ultrason Ferroelectr Freq Control 2004; 51:551–556.

84. Herman BA, Harris GR. Models and regulatory considerations for transient temperature rise during diagnostic ultrasound pulses. Ultrasound Med Biol 2002; 28:1217–1224.

85. Herman BA, Myers MR An analytic derivation for the transient temperature rise during an ultrasound pulse focused on bone. Ultrasound Med Biol 2003; 29:771–773.

86. American Institute of Ultrasound in Medicine, National Electrical Manufacturers Association. Medical Ultrasound Safety. Laurel, MD: American Institute of Ultrasound in Medicine; Rosslyn, VA; National Electrical Manufacturers Association; 1994.